Mech Time-Depend Mater (2015) 19:483–503
DOI 10.1007/s11043-015-9274-8

Quasi-static and dynamic analysis of viscoelastic plates

Ahmet Yalçın Aköz[1] · Fethi Kadıoğlu[2] · Gülçin Tekin[2]

Received: 17 December 2014 / Accepted: 11 July 2015 / Published online: 13 August 2015

Abstract In this study, the quasi-static and dynamic behavior of viscoelastic Kirchhoff plates is studied numerically by using the mixed finite element method in transformed Laplace–Carson space. In the transformed Laplace–Carson space, a new functional has been constructed for viscoelastic Kirchhoff plates through a systematic procedure based on the Gâteaux differential. For numerical inversion, the Maximum Degree of Precision (MDOP), Dubner and Abate's, and Durbin's transform techniques are employed. The developed solution technique is applied to several quasi-static and dynamic example problems.

Keywords Viscoelastic plate · Laplace–Carson transform · Mixed finite element · Inverse Laplace transform

1 Introduction

Plates are one of the most significant structural members due to their wide application in all fields of engineering. The classical (thin) plate theories assume that the material of the plate is linear elastic based on the fundamental assumption of the linear, elastic, small-deflection theory of bending.

Adopting elastic theory to simplify the analysis proves to be inconsistent with reality since most engineering materials exhibit noticeable time-effects due to internal friction. Therefore, viscoelastic constitutive relations should be used instead of elastic constitutive relations with regard to material behavior. There are many works in the literature on the theory of viscoelasticity (Flügge 1975; Christensen 1982).

In structural analysis of time-dependent materials, linear viscoelasticity has been used for a long time. There are basically three approaches that can be used in linear viscoelastic analysis: Laplace transformation, Fourier transformation and Direct Time Integration method

✉ F. Kadıoğlu
fkadioglu@itu.edu.tr

[1] Department of Civil Engineering, Maltepe University, Istanbul, Turkey

[2] Department of Civil Engineering, Istanbul Technical University, Istanbul, Turkey

(Wang and Birgisson 2007; Xu et al. 2004). Flügge (1975) applied Laplace transform to viscoelastic beams. Christensen (1982) presented the application of the Fourier transform to viscoelastic beams. Sorvari and Hämäläinen (2010) analyzed and compared the Time Integration methods in linear viscoelasticity.

Closed-form solutions are often not possible for the problems which have complex geometries, loading conditions and constitutive relations. Hence, numerical solution techniques should be employed. Finite Element Method (FEM) and Boundary Element Method (BEM) are the most commonly used numerical methods in solution of viscoelastic problems. Applications of the FEM to the solution of static and dynamic problems involving materials exhibiting viscoelastic behavior have evolved over a period of time.

The application of the FEM to viscoelastic problems has been presented by a number of authors. White (1986) used constitutive law of hereditary integral type and applied the time interval form finite difference method to perform a finite element analysis in a quasi-static problem. Chen (1995) studied the quasi-static and dynamic response of the linear viscoelastic Timoshenko beam. In the analysis, the hybrid Laplace transform was used to remove the time terms and the FEM was used for the solution of the associated equation. Numerical results were presented and discussed for the Maxwell fluid and three-parameter solid models.

However, to the best of authors' knowledge, there are very few published studies on the analysis of viscoelastic plates. Wang and Tsai (1988) studied the quasi-static and dynamic response of the linear viscoelastic Mindlin plates using the FEM. They used the constitutive law of hereditary integral type and assumed that Poisson ratio is constant. The relaxation modulus is expressed by the Prony series. Yi and Hilton (1994) developed numerical procedures in the time domain using variational principles and a direct time integration method to analyze the transient response of anisotropic viscoelastic composite plates. Ilyasov and Aköz (2000) presented a method to obtain the static and dynamic behavior of viscoelastic triangular plates. The viscoelastic constitutive equations were written in the Boltzmann–Volterra form. Temel and Şahan (2013) investigated the damped response of viscoelastic laminated Mindlin plates using the FEM in conjunction with the Laplace transform method.

When employing the conventional FEM, shear locking is an undesirable phenomenon. In the prevention of shear locking phenomena, reducing the influence of the shear energy by considering suitable Mixed and Non-Standard Finite Element Methods is a more general and flexible way (Lovadina 1996). The use of the Hu–Washizu and Hellinger–Reissner variation principles is more popular when formulating Mixed type Finite Elements. In the work considered here, the Gâteaux Differential Method, which is a more powerful, reliable and efficient variational tool when compared to Hu–Washizu and Hellinger–Reissner variational theorems, is employed to obtain a new functional. Comparison of these techniques is widely discussed by Aköz and Özütok (2000).

Based on the Gâteaux differential, Aköz and Kadıoğlu (1999) constructed two new functionals for viscoelastic Timoshenko beams. For quasi-static and dynamic response of viscoelastic Timoshenko beams, the Mixed Finite Element Method (MFEM) in transformed Laplace–Carson space was used. In addition, Kadıoğlu and Aköz (1999; 2003) developed a functional for the quasi-static and dynamic analysis of viscoelastic circular beams using the MFEM in transformed Laplace–Carson space. Furthermore, Kadıoğlu and Aköz (2000) studied the quasi-static and dynamic responses of linear viscoelastic parabolic beam using the MFEM in the transformed Laplace–Carson space based on the Gâteaux Differential Method. To our knowledge, these are the preliminary studies which have used Laplace–Carson transform to analyze the quasi-static and dynamic response of the viscoelastic beams.

Although the static and dynamic behavior of elastic beam, plate and shell structures is a widely studied topic, there are few studies that exist in the literature pertaining to the

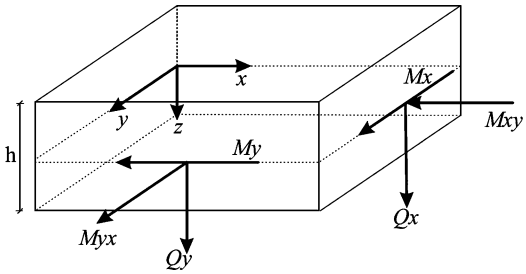

Fig. 1 Internal forces on the laterally loaded rectangular plate element of the middle surface

analysis of the viscoelastic structural elements. To the best of the authors' knowledge, this will be the first study that presents a new functional through a systematic procedure based on the Gâteaux Differential Method for the quasi-static and dynamic analysis of viscoelastic Kirchhoff plates in the Laplace–Carson space.

The unique aspects of this study and the possible contributions of the proposed method to the literature can be explained as follows:

(i) By using this new functional, moment and shear force values that are important for engineers can be obtained directly without any mathematical operation.
(ii) Geometric and dynamic boundary conditions can be obtained easily and a field variable can be included to the functional systematically.
(iii) Shear locking problem can be eliminated by using the Gâteaux Differential Method.

2 Field equation and functional

It is well-known that the constitutive equations of viscoelastic materials for three-dimensional bodies have two different operators for dilatation and distortion. The use of two operators for constitutive equations causes difficulties in solving problems. To overcome these difficulties, two different assumptions are accepted in the literature. In the first assumption, the dilatation is accepted to be elastic, and the distortion viscoelastic. In the second one, the distortion and dilatation parameters are assumed to be equal. The second assumption is equivalent to assuming that the Poisson's ratio is constant. In this study, the second one is accepted (Flügge 1975; Ilioushin and Pobedria 1970).

The field equations of viscoelastic plates are derived considering the equilibrium equations, kinematic relations and viscoelastic constitutive equations as

$$\frac{\partial^2 M_x}{\partial x^2} + \frac{\partial^2 M_y}{\partial y^2} + 2\frac{\partial^2 M_{xy}}{\partial x \partial y} + q = 0 \tag{1}$$

where q indicates the normal load distribution and M_x, M_y, M_{xy} are internal moments. The positive directions of internal forces are illustrated in Fig. 1. The equilibrium equations of a plate can be found in many textbooks such as Timoshenko and Woinowsky-Krieger (1959) and Dym and Shames (1973).

Adopting the Kirchhoff hypothesis, the kinematic relations for plates can be written as follows:

$$\begin{aligned}\varepsilon_x &= -z\frac{\partial^2 w}{\partial x^2},\\ \varepsilon_y &= -z\frac{\partial^2 w}{\partial y^2},\\ \gamma_{xy} &= -2z\frac{\partial^2 w}{\partial x\,\partial y}\end{aligned} \tag{2}$$

where w is the vertical displacement function of the plate's middle surface. To relate the stress–strain (σ–ε) relations, two operators, E_1^* and E_2^* are defined as follows:

$$\begin{aligned}\sigma_x &= E_1^*\varepsilon_x + E_2^*\varepsilon_y,\\ \sigma_y &= E_2^*\varepsilon_x + E_1^*\varepsilon_y.\end{aligned} \tag{3}$$

Using Mohr circle, it can be easily shown that shear stress (τ) and shear strain (γ) relation can be expressed using the same operator as follows:

$$\tau_{xy} = \frac{1}{2}\big(E_1^* - E_2^*\big)\gamma_{xy} \tag{4}$$

where E_1^* and E_2^* can be any operators. Additional details about these operators which are in the hereditary integral form can be obtained from Flügge (1975) in a simple form and obtained from Ilyasov and Aköz (2000) for the plates as follows:

$$\begin{aligned}E_1^* w &= E_{1_{(0)}} w_{(t)} + \int_0^t \frac{dE_{(t-\tau)}}{d(t-\tau)} w_{(\tau)}\,d\tau,\\ E_2^* w &= E_{2_{(0)}} w_{(t)} + \int_0^t \frac{dE_{(t-\tau)}}{d(t-\tau)} w_{(\tau)}\,d\tau.\end{aligned} \tag{5}$$

The bending and torsion moments of plates are obtained as a result of stress as follows:

$$\begin{aligned}M_x &= \int_{-h/2}^{h/2} \sigma_x z\,dz,\\ M_y &= \int_{-h/2}^{h/2} \sigma_y z\,dz,\\ M_{xy} &= \int_{-h/2}^{h/2} \tau_{xy} z\,dz.\end{aligned} \tag{6}$$

Substituting Eqs. (2)–(4) into Eq. (6) and carrying out integration, we get

$$\begin{aligned}M_x &= -\frac{h^3}{12}\left[E_1^*\frac{\partial^2 w}{\partial x^2} + E_2^*\frac{\partial^2 w}{\partial y^2}\right],\\ M_y &= -\frac{h^3}{12}\left[E_1^*\frac{\partial^2 w}{\partial y^2} + E_2^*\frac{\partial^2 w}{\partial x^2}\right],\\ M_{xy} &= -\frac{h^3}{12}\big[E_1^* - E_2^*\big]\frac{\partial^2 w}{\partial x\,\partial y}.\end{aligned} \tag{7}$$

If a new operator D^* is defined as

$$D^* = \frac{h^3}{12} E_1^* \tag{8}$$

and the second assumption is adopted, Eq. (7) can be written as follows:

$$\begin{aligned} M_x &= -D^* \left[\frac{\partial^2 w}{\partial x^2} + \nu \frac{\partial^2 w}{\partial y^2} \right], \\ M_y &= -D^* \left[\frac{\partial^2 w}{\partial y^2} + \nu \frac{\partial^2 w}{\partial x^2} \right], \\ M_{xy} &= -(1-\nu) D^* \frac{\partial^2 w}{\partial x \partial y} \end{aligned} \tag{9}$$

where ν is Poisson's ratio and D^* is the operator form of the flexural rigidity of the plate.

In order to remove the time derivatives from governing equations and boundary conditions, the method of Laplace–Carson transform will be employed. The Laplace–Carson transform of a real function is

$$\bar{f}_{(s)} = s f_{(s)} \tag{10}$$

where the Laplace transform of a real function is:

$$\begin{aligned} f_{(s)} &= L[f_{(t)}] = \int_0^\infty e^{-st} f_{(t)}\, dt, \\ f_{(t)} &= L^{-1}[f_{(s)}] = \frac{1}{2\pi i} \int_{a-i\infty}^{a+i\infty} e^{st} f_{(s)}\, ds. \end{aligned} \tag{11}$$

Taking Laplace–Carson transform of Eqs. (1) and (9), we obtain the field equations in Laplace–Carson space:

$$\begin{aligned} -\frac{\partial^2 \bar{M}_x}{\partial x^2} - \frac{\partial^2 \bar{M}_y}{\partial y^2} - 2\frac{\partial^2 \bar{M}_{xy}}{\partial x \partial y} &= \bar{q}, \\ -\bar{M}_x - \bar{D}^* \left(\frac{\partial^2 \bar{w}}{\partial x^2} + \nu \frac{\partial^2 \bar{w}}{\partial y^2} \right) &= 0, \\ -\bar{M}_y - \bar{D}^* \left(\frac{\partial^2 \bar{w}}{\partial y^2} + \nu \frac{\partial^2 \bar{w}}{\partial x^2} \right) &= 0, \\ -\bar{M}_{xy} - (1-\nu) \bar{D}^* \frac{\partial^2 \bar{w}}{\partial x \partial y} &= 0 \end{aligned} \tag{12}$$

where $\bar{D}^*$ is related with the creep function $\bar{Y}^*$ as follows:

$$\bar{D}^* = \frac{h^3}{12} \bar{Y}^*. \tag{13}$$

To complete the field equations, the boundary conditions are defined as follows:

$$\begin{aligned} \bar{T} &= \hat{\bar{T}}, \\ -\bar{M} &= -\hat{\bar{M}}, \end{aligned} \qquad \text{(Dynamic Boundary Condition)} \tag{14}$$

$$\begin{aligned} \bar{w}' &= \hat{\bar{w}}', \\ -\bar{w} &= -\hat{\bar{w}} \end{aligned} \quad \text{(Geometric Boundary Condition)} \tag{15}$$

where the quantities with hat are given at the boundary points. Of course, these boundary conditions do not belong to a specific problem and they serve to include boundary terms to the functional.

These equations can be written in operator form similar to elastic plate as (see Aköz and Özçelikörs 1985 for a review)

$$\bar{\boldsymbol{Q}} = \bar{\boldsymbol{P}}\bar{\boldsymbol{u}} - \bar{\boldsymbol{f}}. \tag{16}$$

The explicit form of operator $\boldsymbol{Q}$ in the Laplace–Carson space is given in the Appendix. If the operator $\boldsymbol{Q}$ is potential (Oden and Reddy 1976) then

$$\left\langle d\,\bar{\boldsymbol{Q}}\left(\bar{\boldsymbol{u}}, \bar{\boldsymbol{u}}'\right), \bar{\boldsymbol{u}}^*\right\rangle = \left\langle d\,\bar{\boldsymbol{Q}}\left(\bar{\boldsymbol{u}}, \bar{\boldsymbol{u}}^*\right), \bar{\boldsymbol{u}}'\right\rangle \tag{17}$$

must be satisfied. After satisfying the requirement, the functional is obtained as

$$I(\bar{\boldsymbol{u}}) = \int_0^1 \left\langle \bar{\boldsymbol{Q}}(\eta\bar{\boldsymbol{u}}, \bar{\boldsymbol{f}}), \bar{\boldsymbol{u}}\right\rangle d\eta. \tag{18}$$

Inserting Eq. (16) into Eq. (18), the functional for viscoelastic Kirchhoff plate is obtained as follows:

$$\begin{aligned} I(\bar{\boldsymbol{u}}) = &\left[\frac{\partial\bar{w}}{\partial x}, \frac{\partial\bar{M}_x}{\partial x}\right] + \left[\frac{\partial\bar{w}}{\partial y}, \frac{\partial\bar{M}_y}{\partial y}\right] + \left[\frac{\partial\bar{w}}{\partial x}, \frac{\partial\bar{M}_{xy}}{\partial y}\right] + \left[\frac{\partial\bar{w}}{\partial y}, \frac{\partial\bar{M}_{xy}}{\partial x}\right] - [\bar{q}, \bar{w}] \\ &- \frac{1}{2\bar{D}(1-\nu^2)}[\bar{M}_x, \bar{M}_x] - \frac{1}{2\bar{D}(1-\nu^2)}[\bar{M}_y, \bar{M}_y] + \frac{\nu}{\bar{D}(1-\nu^2)}[\bar{M}_x, \bar{M}_y] \\ &- \frac{1}{\bar{D}(1-\nu)}[\bar{M}_{xy}, \bar{M}_{xy}] - [\hat{\bar{T}}, \bar{w}]_\sigma - \left[(\bar{M} - \hat{\bar{M}}), \bar{w}'\right]_\sigma \\ &- \left[\hat{\bar{w}}', \bar{M}\right]_\varepsilon - \left[(\bar{w} - \hat{\bar{w}}), \bar{T}\right]_\varepsilon \end{aligned} \tag{19}$$

where [,] is the inner product which is defined as

$$[f, g] = \int_A fg\,dA. \tag{20}$$

Using the functional in Eq. (19), viscoelastic plate element VPLT16 can be obtained with four nodal variables $\bar{w}$, $\bar{M}_x$, $\bar{M}_y$, $\bar{M}_{xy}$. In Eq. (19), the last four terms are boundary conditions defined as:

$$\begin{aligned} [\bar{T}, \bar{w}] &= \left[\left(\frac{\partial\bar{M}_x}{\partial x} + \frac{\partial\bar{M}_{xy}}{\partial y}\right)n_x + \left(\frac{\partial\bar{M}_y}{\partial y} + \frac{\partial\bar{M}_{xy}}{\partial x}\right)n_y, \bar{w}\right], \\ \left[\bar{M}, \bar{w}'\right] &= [\bar{M}_x, \bar{w}_{,x}n_x] + [\bar{M}_y, \bar{w}_{,y}n_y] + \left[\bar{M}_{xy}, (\bar{w}_{,x}n_y + \bar{w}_{,y}n_x)\right]. \end{aligned} \tag{21}$$

Equation (21) shows the work done by the shear force at the boundary and the work done by the moment force at the boundary, respectively.

Fig. 2 Master element

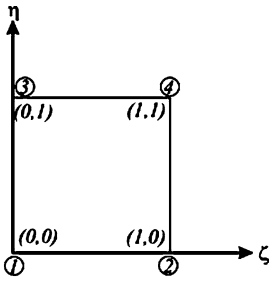

Fig. 3 Rectangular element

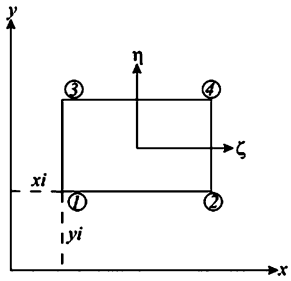

3 Finite element formulation of viscoelastic Kirchhoff plates

The functional variables $\bar{w}$, $\bar{M}_x$, $\bar{M}_y$, $\bar{M}_{xy}$ in Eq. (19) are in the Laplace–Carson space. Therefore, the finite element formulation belongs to the same space. To derive the finite element formulation, first the interpolation function must be chosen. The regularity of the shape function, N, depends on the maximum degree of derivatives in the functional. To have rigorous assurance of convergence as element size decreases, we must satisfy compatibility and completeness requirement. Since the first derivative of the variables exists in the functional in Eq. (19), conforming element formulation for the shape function must satisfy $C^{\circ}(r)$ continuity at element boundary and $C'(\Omega)$ continuity in element; see Huebner (1975).

Rectangular master element is used in the formulation, see Fig. 2. The shape function for the element is

$$\begin{aligned} N_1 &= (1-\xi)(1-\eta), \\ N_2 &= \xi(1-\eta), \\ N_3 &= (1-\xi)\eta, \\ N_4 &= \xi\eta. \end{aligned} \tag{22}$$

For arbitrary geometry, general coordinate transformation between (x, y) and (ξ, η) coordinate systems is defined by:

$$\begin{aligned} x &= \sum x_i N_i(\xi, \eta), \\ y &= \sum y_i N_i(\xi, \eta) \end{aligned} \tag{23}$$

where $N = 4$ for the rectangular element (as in Fig. 3).

The four variables of the functional given in Eq. (19) are expressed by the shape function N_i in the element as follows:

$$\begin{aligned}
\bar{w} &= \sum_{i=1}^{4} \bar{w}_i N_i(\xi, \eta), \\
\bar{M}_x &= \sum_{i=1}^{4} \bar{K}_i N_i(\xi, \eta), \\
\bar{M}_y &= \sum_{i=1}^{4} \bar{M}_i N_i(\xi, \eta), \\
\bar{M}_{xy} &= \sum_{i=1}^{4} \bar{L}_i N_i(\xi, \eta)
\end{aligned} \tag{24}$$

where $\bar{w}$, $\bar{K}$, $\bar{M}$ and $\bar{L}$ correspond to nodal variables, $\bar{w}$, $\bar{M}_x$, $\bar{M}_y$ and $\bar{M}_{xy}$ respectively.

All expressions of unknown and known quantities in terms of interpolation functions are inserted into Eq. (19) and, simplifying with respect to nodal variables; the following element matrix is derived for the VPLT16 element based on the submatrices ($[k_1]$, $[k_2]$, $[k_3]$ and $[k_4]$) of the rectangular finite element:

$$\begin{pmatrix} 0 & k_2 & k_3 & k_4 \\ k_2 & -\alpha k_1 & \alpha\nu k_1 & 0 \\ k_3 & \alpha\nu k_1 & -\alpha k_1 & 0 \\ k_4 & 0 & 0 & -\beta k_1 \end{pmatrix} \begin{pmatrix} \bar{w} \\ \bar{K} \\ \bar{M} \\ \bar{L} \end{pmatrix} = \begin{pmatrix} k_1\bar{q} \\ 0 \\ 0 \\ 0 \end{pmatrix} \tag{25}$$

where

$$\begin{aligned}
\alpha &= \frac{1}{\bar{D}(1-\nu^2)}, \\
\beta &= \frac{1}{2\bar{D}(1-\nu)}.
\end{aligned} \tag{26}$$

4 Numerical inversion of FEM solution

FEM formulation of viscoelastic Kirchhoff plate is derived in Laplace–Carson space, and the numerical solution is obtained for different numerical values of transform parameters. In order to obtain the solution in the real time domain, the inverse transformation is necessary. There exist various methods for the inverse numerical Laplace transformation. The classification of Laplace inversion techniques is given by Aral and Gülçat (1977). For a discussion of Laplace inversion process, see Dubner and Abate (1968), Krylov and Skoblya (1969), Durbin (1974), Narayanan and Beskos (1982).

In this study, we have restricted ourselves to the Maximum Degree of Precision (MDOP), Durbin's, and Dubner and Abate's methods.

In the MDOP method, the function can be approximated by quadrature as

$$f_{(t)} = \frac{1}{t} \sum_{k=1}^{n} W^k S_k^m \left[F\left(\frac{S_k}{t}\right) \right] \tag{27}$$

where S_k is the abscissa and W^k is the weight function. Weights are taken from Krylov and Skoblya (1969). In this study, calculation are carried out for $m = 1$ and $n = 5$.

In Dubner and Abate's method, $f(t)$ is assumed to be expanded in a series of orthogonal polynomials $\Phi(t)$, as:

$$f_{(t)} = \sum_{k=0}^{\infty} C_k \Phi_k(t). \tag{28}$$

The coefficients C_k are then expressed in terms of the values of $f(s)$ at certain real points, and we end up with:

$$f_{(t)} = \frac{2e^{at}}{T}\left\{\frac{1}{2}\mathrm{Re}\big[F(a)\big] + \sum_{k=1}^{\infty}\mathrm{Re}\left[F\left(a + \frac{k\pi i}{T}\right)\right]\cos\left(\frac{k\pi}{T}t\right)\right\}. \tag{29}$$

If we substitute $aT = A$ and $T = 2t$ in Eq. (29), we obtain

$$f_{(t)} = \frac{e^{\frac{A}{2}}}{t}\left\{\frac{1}{2}F\left(\frac{A}{2t}\right) + \sum_{n=1}^{\infty}(-1)^n\,\mathrm{Re}\left[F\left(\frac{A + 2n\pi i}{2t}\right)\right]\right\}. \tag{30}$$

In the computer program, Eq. (29) is employed.

Durbin's method is an efficient improvement of Dubner and Abate's method. Durbin combined both finite Fourier Sine and Cosine transforms to obtain the inversion formula as

$$f_{(t_j)} = \frac{2e^{aj\Delta t}}{T}\left\{-\frac{1}{2}\mathrm{Re}\big[F(a)\big] + \mathrm{Re}\left[\sum_{k=0}^{N-1} L_k\left(A_{(k)} + iB_{(k)}\right)\right]W^{jk}\right\} \tag{31}$$

where

$$\begin{aligned}
A_{(k)} &= \sum_{p=0}^{L}\mathrm{Re}\left[F\left(a + i(k + pN)\frac{2\pi}{N}\right)\right],\\
B_{(k)} &= \sum_{p=0}^{L}\mathrm{Im}\left[F\left(a + i(k + pN)\frac{2\pi}{N}\right)\right],\\
W &= \cos\left(\frac{2\pi}{N}\right) + i\sin\left(\frac{2\pi}{N}\right),\\
L_k &= \frac{\sin(\frac{k\pi}{N})}{(\frac{k\pi}{N})}.
\end{aligned} \tag{32}$$

A computer program was written for the above inversion methods. The results of these methods are discussed in applications.

5 Numerical solution

The method performance is tested through various problems presented below. In all applications, Kelvin or Three-parameter Kelvin (TPK) model is employed.

These models are represented by a spring–dashpot elements as illustrated in Fig. 4. The displacement of Kelvin and Three-parameter Kelvin models approaches a finite value as

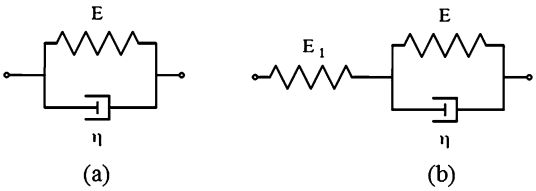

Fig. 4 Mechanical analog for the Kelvin (**a**) and Three-parameter Kelvin (**b**) model

$t \to \infty$. Kelvin model does not have an elastic response to the suddenly applied load, but the Three-parameter Kelvin model has an elastic response for $t = 0$.

The material coefficients are chosen as follows:

- The Kelvin model:

$$E = 3 \times 10^7 \text{ kPa}, \qquad \eta = 3 \times 10^7 \text{ kPa s}, \qquad \nu = 0.3;$$

- The Three-parameter solid model:

$$E_1 = 3 \times 10^7 \text{ kPa}, \qquad E = 3 \times 10^7 \text{ kPa}, \qquad \eta = 3 \times 10^7 \text{ kPa s}, \qquad \nu = 0.3.$$

The relaxation modulus of Kelvin and Three-parameter Kelvin material are as follows:

$$\begin{aligned} J_{(t)} &= \frac{1}{E}\left(1 - e^{-\frac{E}{\eta}t}\right), \\ J_{(t)} &= \frac{1}{E_1} + \frac{1}{E}\left(1 - e^{-\frac{E}{\eta}t}\right). \end{aligned} \tag{33}$$

In all applications, the quarter of simply supported rectangular plate with length $a = 4$ m, width $b = 4$ m and thickness $h = 0.1$ m as illustrated in Fig. 5 is solved for different loads. The displacement and time are measured in meters (m) and seconds (s), respectively. In all numerical examples, the displacement value is given for the middle point of the plate by

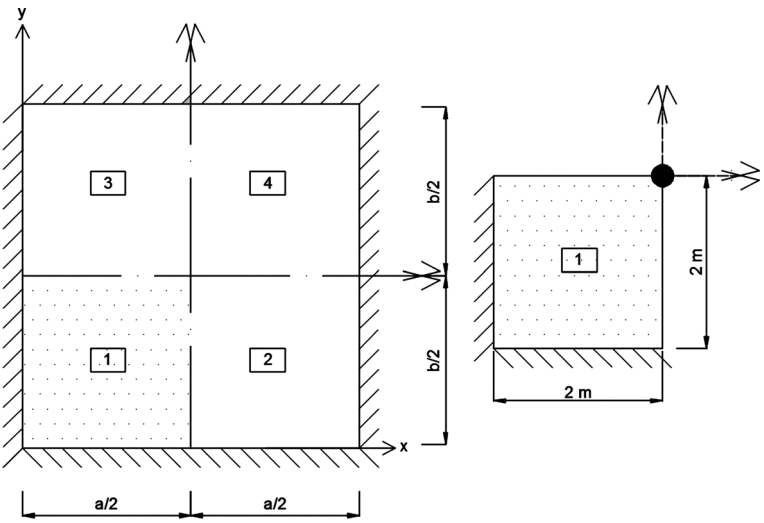

Fig. 5 Geometrical properties of the simply supported rectangular plate

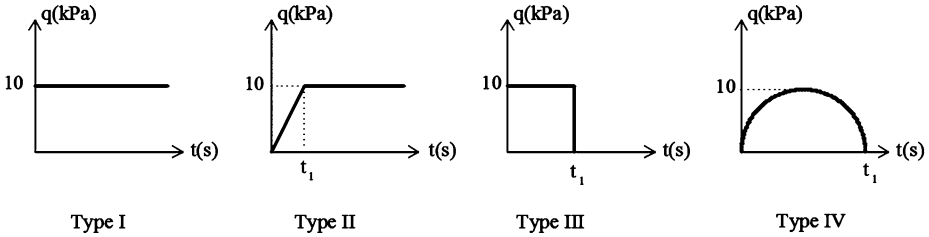

Fig. 6 Time histories of external loads

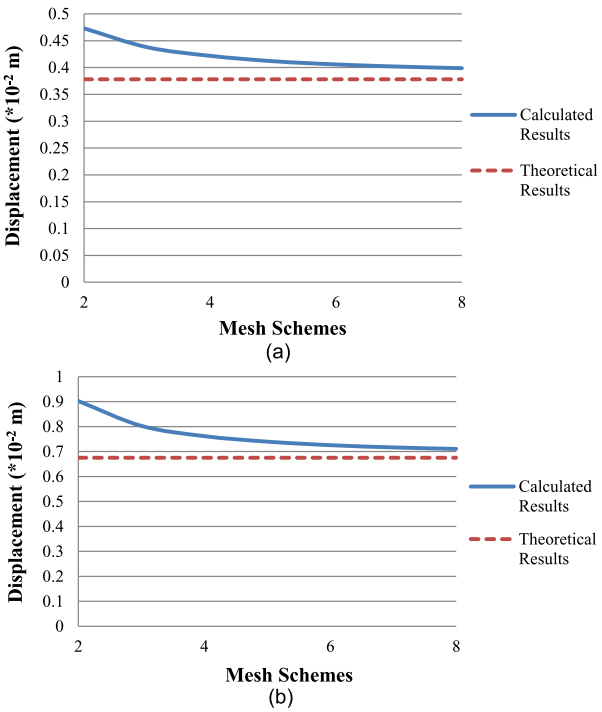

Fig. 7 Comparison of theoretical and calculated deflection results under (**a**) step load, (**b**) point load

taking advantage of the symmetry property. The time histories of loads in applications are sketched in Fig. 6.

Using different types of time-dependent loads and viscoelastic material models enhances the accuracy and applicability of the presented results for subsequent studies.

Example 1 The performance of the developed computer program is tested through this example. This program consists of two parts, elastic and viscoelastic. In this example, the elastic part is tested.

A plate is subjected to a Type I load (step load) of $q_o = 10$ kPa and a point load $P = 100$ kN separately. The displacement values at the center of the elastic plate are computed for different orders of mesh schemes, 2×2, 4×4, 6×6 and 8×8, and the results are presented in Fig. 7(a)–(b). The results are compared with existing results in the literature in order to determine the most suitable mesh scheme.

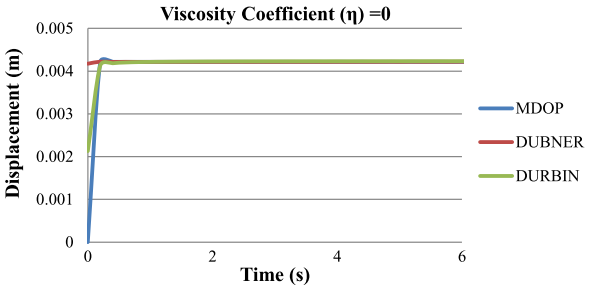

Fig. 8 The displacement-time variation of the center point of an elastic plate

Simulations show that if the mesh gets finer, the results of the developed mixed finite element solution show good agreement with the theoretical results. However, an increase in the number of mesh cells naturally increases the time of computer solution.

As illustrated in Fig. 7, the 4×4 mesh scheme results are very satisfactory and this scheme has the advantage of saving time. Therefore, through this study, the results of the 4×4 mesh scheme are considered in all numerical examples. For the theoretical results of elastic plates, see Timoshenko and Woinowsky-Krieger (1959).

Once the results of elastic plates and the most suitable mesh scheme for the solution are obtained, the performance of the viscoelastic part of the developed program is tested for the elastic plates.

In this example, the viscoelastic coefficient, η, is set to zero in the developed viscoelastic computer program in order to obtain the results of the elastic plate. The results of the elastic plates obtained from the developed mixed finite element viscoelastic Kirchhoff plate program are given in Fig. 8 for the step load (Type I). The numerical results show an excellent agreement with the theoretical results of elastic plates. Thus, it is proved that the performance of the developed viscoelastic computer program is efficient.

Example 2 The main objective of this example is to determine the most suitable values for the effective parameters of the inverse transform techniques. As the value of aT is changed, fluctuation is observed in Dubner and Abate's and Durbin's inverse transform techniques. In addition to aT, the results depend also on parameter N. The error in the solution decreases as the value of N increases. This example is solved for a Kelvin solid employing MDOP, Dubner and Abate's and Durbin's inverse transform techniques for different values of aT ($aT = 5$, 10 and 20, respectively). The time variation of the bending moment and displacement of the center point under the Type I load are computed. The results are presented in Fig. 9. It is observed that the results of the MDOP method are independent of aT. However, fluctuation is observed in the Dubner and Abate's and Durbin inverse transform methods when aT takes values bigger than 10. As observed from Fig. 9, the fluctuation scattering increases as aT in Dubner and Abate's inverse transform technique increases. Fluctuation is observed for $t > 20$ s as $aT = 20$ and for $t > 30$ s as $aT = 10$ in Dubner and Abate's and Durbin's methods. If the time histories of the external loads in applications are considered, it is clearly seen that the behavior up to maximum 10 seconds is our interest. So throughout this study, all examples are solved for the values of aT less than or equal to 10. For the next examples, problems are solved for $aT = 5$ or 10 and $N = 100$ or 200 to decrease the fluctuation and the error in the solutions.

Example 3 A plate is subjected to different loads, and the time histories are illustrated in Fig. 6. Kelvin solid model is employed. For the numerical inversion, the MDOP, Dubner

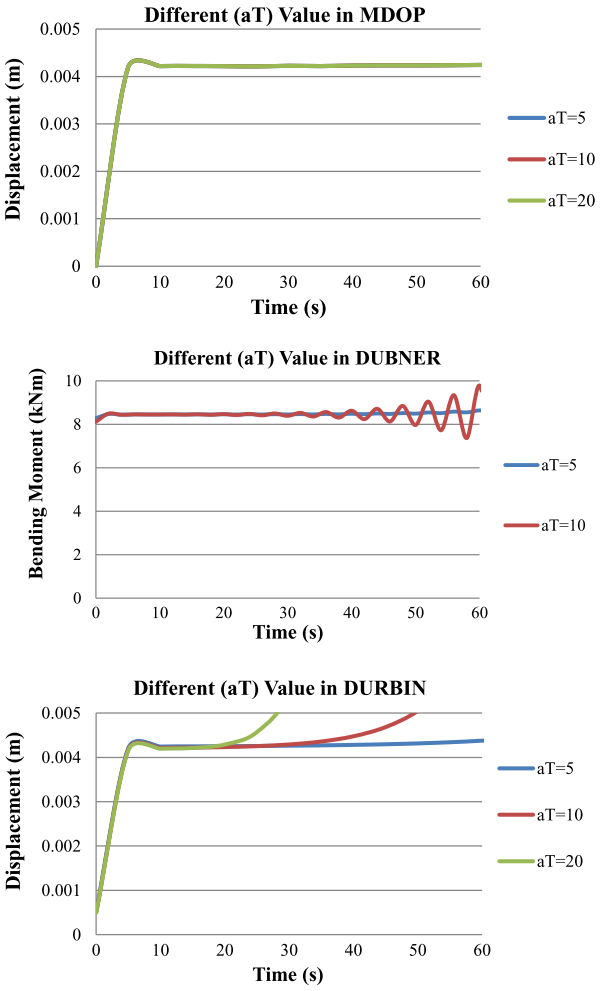

Fig. 9 Effect of the changes in the value of the aT parameter

and Abate's and Durbin's transform techniques are used. The time-dependent displacement and bending moment at the center of the plate are computed and presented in Fig. 10. This example is solved for the η (viscosity coefficient of the material)/E (modulus of elasticity of the material) ratio being equal to one.

The success of the MDOP, Dubner and Abate's and Durbin's methods is tested for the step load (Type I), gradual step load for $t_1 = 2$ s (Type II), rectangular impulsive load for $t_1 = 10$ s (Type III) and sinusoidal impulsive load $t_1 = 10$ s (Type IV). It is observed that the MDOP method gives good results for the displacement variation as compared to the bending moment variation. Fluctuation is observed in the time-dependent bending moment at the center of the plate as time increases in the MDOP inverse transform technique. Therefore, the time variation of the bending moment is presented only for the Dubner and Abate's and Durbin's inverse transform methods.

When the time variation of the bending moment at the center point is considered, it is observed that Durbin's method gives perfect results compared to Dubner and Abate's

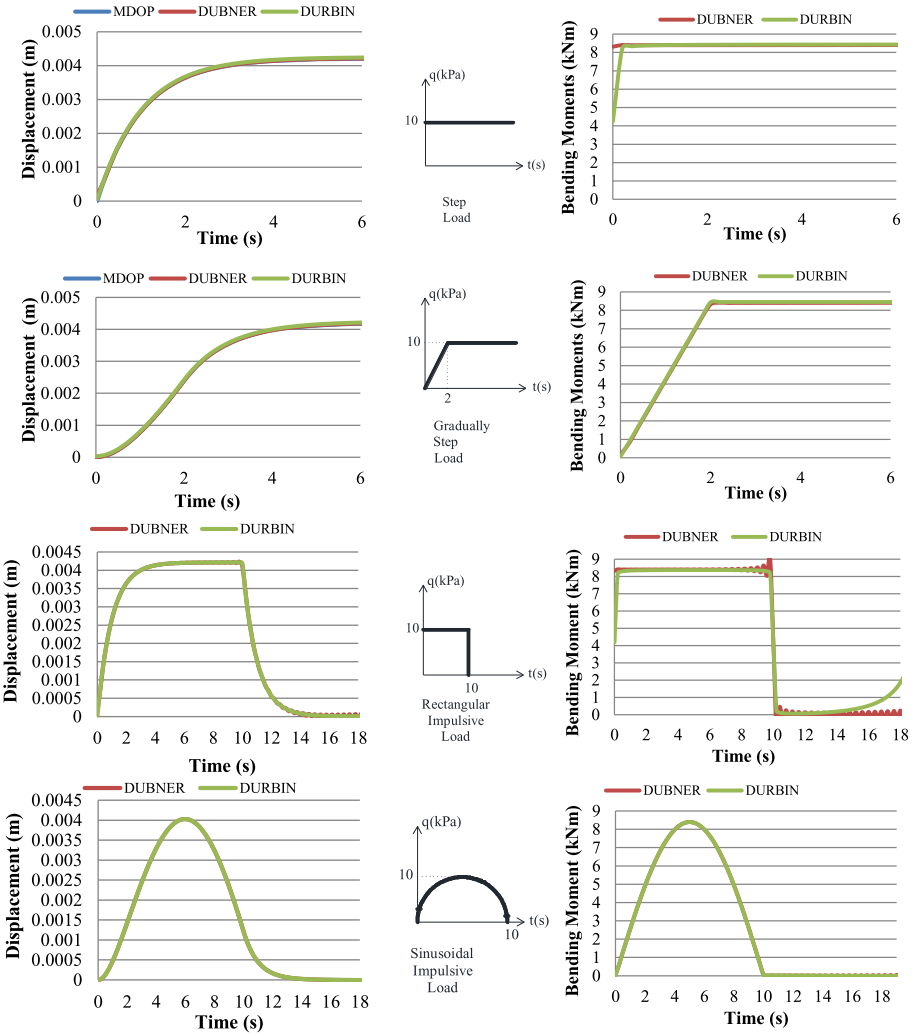

Fig. 10 The displacement and bending moment-time variation results for the damping ratio $\eta/E = 1$

method for the Type III and IV loads. Since little fluctuation exists in the Dubner and Abate's method as time increases, the results are not shown in the next examples.

Example 4 The problem is solved for a Kelvin solid employing different η/E ratios in order to show the damping effect in displacement variation of the center point. When the viscosity coefficient decreases, the time-dependent displacement behavior of the plate approaches the elastic behavior as expected. The results are given in Fig. 11 only for the rectangular impulsive load (Type III) employing Durbin's inverse transform technique.

Example 5 This example is solved for a Three-parameter Kelvin Solid (TPK) under the Type III load employing Durbin's inverse Laplace transform technique. The time-dependent displacement at the center of the plate is presented in Fig. 12 for the damping ratio (η/E)

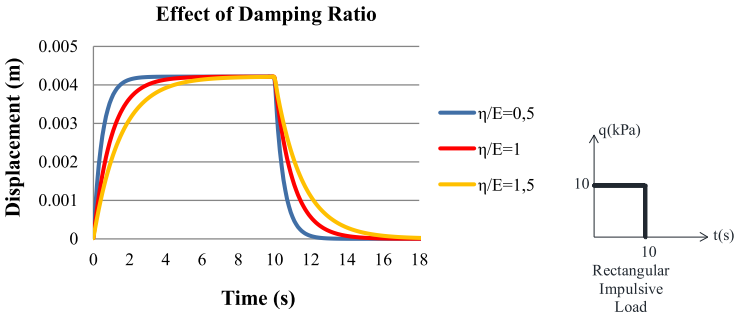

Fig. 11 Effect of the different η/E ratios

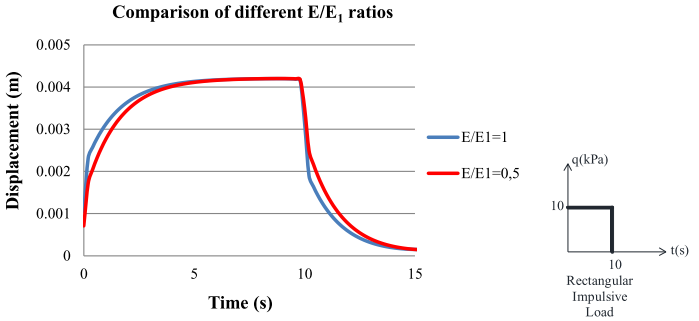

Fig. 12 Variation of different E/E_1 ratio curves when the damping ratio equals to 1.5

equal to 1.5. The results are presented for different E/E_1 ratios, and the time-dependent displacements are compared with the previous example's results (the curve corresponds to the damping ratio equal to 1.5). As expected, the E/E_1 ratio increases as the E_1 value of TPK decreases, and the results of the TPK model coincide with those for the Kelvin solid model.

Example 6 In this example, the dynamic response of a simply supported viscoelastic plate ($a = b = 2$ m and $h = 0.1$ m) is considered. For the analysis, the Kelvin solid model is employed. The problem is solved for the Type I load, using the MDOP, Dubner and Abate's and Durbin's inverse transform techniques. The material density ρ is defined as the mass density per unit volume of the plate, and it is assumed to be 2000 kg/m^3; and we also take $E = 3 \times 10^7$ kPa. In order to determine the frequency of vibration, free vibration analysis is carried out for ($m = 1$ and $n = 1$). The effect of the increasing viscosity coefficient η on the transient response and the frequency of vibration is shown in Fig. 13. When η is assumed to be 1500 kPa s, the vibration period, T, of the plate equals to 0.0435 s. The vibration behavior of the viscoelastic plate resembles the vibration of an elastic plate for small values of the viscosity coefficient. This result is compared with the existing studies done by Leissa (1969) and Craig and Kurdila (2006) and provides theoretical validation for the use of the vibration frequency of elastic plates (see Eq. (34) for a review):

$$\omega = \sqrt{\frac{D}{\rho h}\left[\left(\frac{m\pi}{a}\right)^2 + \left(\frac{n\pi}{b}\right)^2\right]} \tag{34}$$

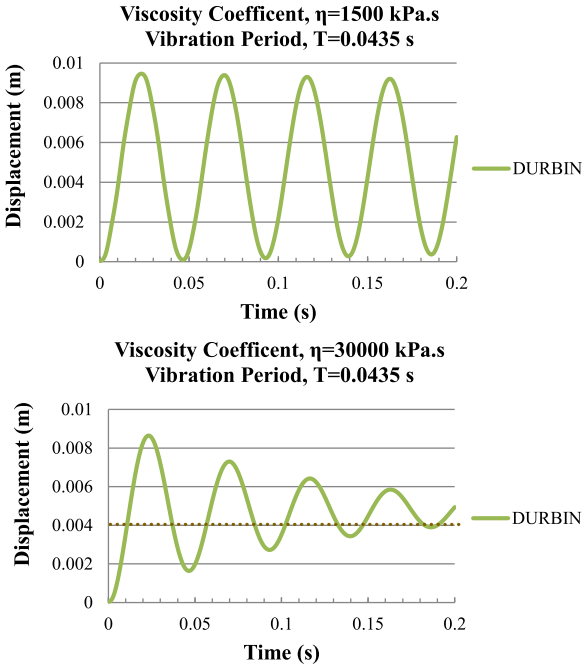

Fig. 13 Effect of viscosity coefficient on the vibration period and amplitude of displacement

where

$$D = \frac{Eh^3}{12(1-\nu^2)}. \tag{35}$$

If D is substituted in Eq. (34), then

$$\omega = \frac{2\pi}{T} = h\sqrt{\frac{E}{12(1-\nu^2)\rho}}\left[\left(\frac{m\pi}{a}\right)^2 + \left(\frac{n\pi}{b}\right)^2\right] \tag{36}$$

is obtained.

When the viscosity coefficient is assumed to be 30 000 kPa s, the viscoelastic plate shows vibration in the same period as the elastic plate, and the time behavior under the Type I load is illustrated in Fig. 13. As it is known, the period of vibration depends on the viscosity coefficient, and a change in the value of free vibration period is expected when the viscosity coefficient is increased. However, it is observed that when the viscosity coefficient takes any value between 1500 and 30 000, the viscoelastic plate will vibrate in the same period as the elastic plate.

Moreover, this example shows the effect of the thickness variation on the dynamic behavior of the viscoelastic plates. The material density ρ is taken as 2000 kg/m^3, η is assumed to be 1500 kPa s, and $E = 3 \times 10^7$ kPa. The thickness of the plate, h, is assumed as 0.01 m. The results are presented in Fig. 14. It is observed that decreasing the thickness of the plate element does not cause shear locking.

In addition, the vibration period is inversely proportional to the thickness, as expected. If the thickness of the plate is changed from 0.1 m (the results are presented in Fig. 13(a)) to 0.01 m, according to Eq. (36), the vibration period of the plate becomes $T_1 = 10$ T and equals to 0.435 s as seen in Fig. 14. This is a very important result to show that the new

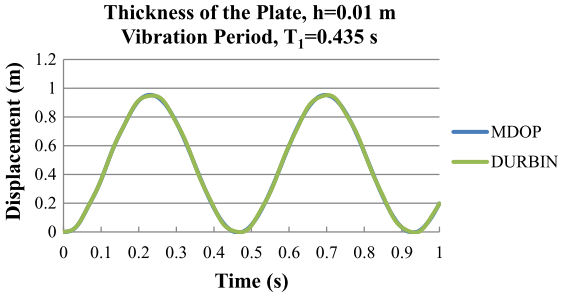

Fig. 14 Effect of plate thickness on the vibration period and amplitude of displacement

solution method is free from shear locking. It is impossible to obtain similar results using the well-known classical finite element method (see Bathe 1982 and Reddy 1993).

Example 7 In this example, the problem is solved for the Kelvin solid model employing Dubner and Abate's and Durbin's inverse transform techniques. The material density ρ is assumed as 2000 kg/m^3, the viscosity coefficient η is assumed as 3000 kPa s, and $E = 3 \times 10^5$ kPa. The dynamic behavior of the viscoelastic plate under the rectangular impulsive load is illustrated in Fig. 15. The time-dependent displacement amplitude at the center of the plate is continuous, whereas their derivatives show discontinuity at the time the load is removed ($t = 1$ s). When $t > 1$ s, the plate starts to vibrate in the reverse direction.

Example 8 In this example, the problem is solved for the Kelvin solid model employing Durbin's inverse transform technique. A viscoelastic plate is subjected to a point load $P = 100$ kN. The displacement values at the center of the viscoelastic plate are computed for the 4×4 mesh scheme. The results of the developed mixed finite element viscoelastic Kirchhoff plate program and the theoretical results of viscoelastic plates under point load are presented in Fig. 16. The numerical results show an excellent agreement with the theoretical results of viscoelastic plates. Thus, it is proved that the performance of the developed viscoelastic computer program is efficient.

Moreover, in this example different η/E ratios are considered in order to show the damping effect in displacement variation of the center point of the viscoelastic plate under point load $P = 100$ kN. The results are given in Fig. 17.

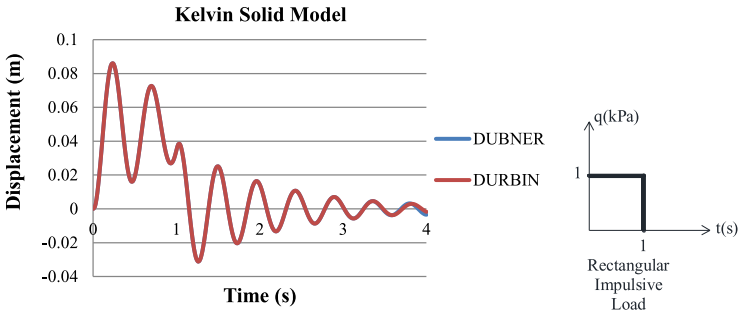

Fig. 15 Dynamic behavior of Kelvin solid model

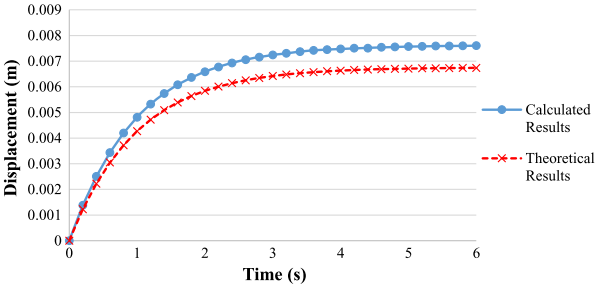

Fig. 16 Comparison of theoretical and calculated deflection results of viscoelastic plates under point load

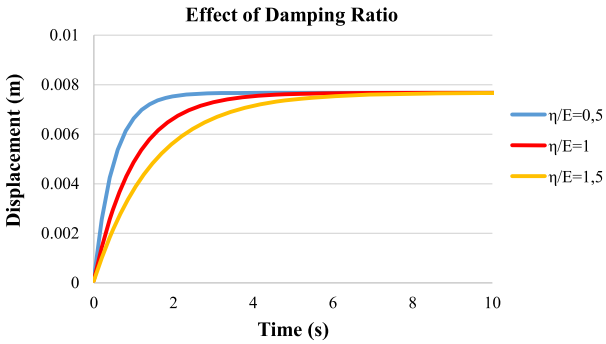

Fig. 17 Effect of the different η/E ratios under point load

6 Conclusion

In a one dimensional problem such as bending or torsion of bars, one constitutive constant is required. In isotropic plate problems, the constitutive equation of viscoelastic materials has two different operators for dilatation and distortion. The use of two operators causes difficulties in solving problems. To overcome these difficulties, two simplifying assumptions are accepted in the literature. According to the first assumption, the dilatation is elastic and the distortion is viscoelastic. According to the second one, the distortion and dilatation parameters are proportional. The second assumption is equivalent to assuming that the Poisson ratio is constant. In this study, employing the second assumption,

(i) The field equations of Kirchhoff plates in Laplace–Carson space have been obtained.
(ii) A new functional has been constructed for viscoelastic Kirchhoff plates in Laplace–Carson space through a systematic procedure based on the Gâteaux differential. The functional has four independent variables, $\bar{w}$, $\bar{M}_x$, $\bar{M}_y$, $\bar{M}_{xy}$, in Laplace–Carson space.
(iii) Also, geometric (essential) and dynamic (natural) boundary conditions have been obtained.
(iv) A special mixed finite element program has been written which has four independent field variables. Since the first derivatives of the variables exist in the functional, the conforming element formulation for the shape function N must satisfy only $C^0(r)$ continuity.
(v) To transform the numerical results from Laplace–Carson space, various transform techniques have been tested. In particular, the MDOP, Dubner and Abate and Durbin methods have been employed. The performance of the methods has been tested through various quasi-static and dynamic problems.
(vi) The results are quite in agreement with each other for a simply supported plate. The calculation is accomplished for different mesh Ωh, beginning with 2×2 and ending

with 8×8. The error in the energy norm satisfies the inequality $e < ch^p$ as presented by Reddy (1993), where c is a constant and h is the characteristic element length.

(vii) The free vibration period of a viscoelastic plate has been obtained by the proposed mixed finite element model.

(viii) A viscoelastic plate vibrates in the same period as does elastic plate for small values of viscosity coefficient, as expected.

(ix) The free vibration period of a simply supported viscoelastic plate is inversely proportional to the thickness. Results are in good agreement with the periods of elastic plates in the literature for all thicknesses. This presented formulation avoids shear locking.

(x) In this study, a new mixed finite element is developed for viscoelastic Kirchhoff plates, utilizing the new functional through standard procedures (see Kadıoğlu and Aköz 2003; Aköz and Kadıoğlu 1999 and Aköz and Özütok 2000). The same approach can be applied for the higher order plate theories as well as shell theories. Following the described methodology, some of these problems are under study.

Acknowledgements This research is supported by the Scientific and Technological Research Council of Turkey under the grant number 213M332 and by the Research Foundation of Istanbul Technical University (ITU) under grant number 37961. The authors gratefully acknowledge this support.

Appendix

The operator form of field equations $\bar{\boldsymbol{Q}} = \bar{\boldsymbol{P}}\bar{\boldsymbol{u}} - \bar{\boldsymbol{f}}$ in the Laplace–Carson space is

$$\begin{bmatrix} 0 & \bar{P}_{12} & \bar{P}_{13} & \bar{P}_{14} & 0 & 0 & 0 & 0 \\ \bar{P}_{21} & \bar{P}_{22} & \bar{P}_{23} & 0 & 0 & 0 & 0 & 0 \\ \bar{P}_{31} & \bar{P}_{32} & \bar{P}_{33} & 0 & 0 & 0 & 0 & 0 \\ \bar{P}_{41} & 0 & 0 & \bar{P}_{44} & 0 & 0 & 0 & 0 \\ 0 & 0 & 0 & 0 & 0 & 0 & 0 & 1 \\ 0 & 0 & 0 & 0 & 0 & 0 & -1 & 0 \\ 0 & 0 & 0 & 0 & 0 & 1 & 0 & 0 \\ 0 & 0 & 0 & 0 & -1 & 0 & 0 & 0 \end{bmatrix} \begin{bmatrix} \bar{w} \\ \bar{u}_2 \\ \bar{u}_3 \\ \bar{u}_4 \\ \bar{w}_0 \\ \bar{w}_0' \\ \bar{M} \\ \bar{T} \end{bmatrix} = \begin{bmatrix} \bar{q} \\ 0 \\ 0 \\ 0 \\ \hat{\bar{T}} \\ -\hat{\bar{M}} \\ \hat{\bar{w}}' \\ -\hat{\bar{w}} \end{bmatrix} \tag{A.1}$$

where

$$\begin{aligned} \bar{P}_{12} &= -\bar{D}\left(\frac{\partial^2}{\partial x^2} + \nu\frac{\partial^2}{\partial y^2}\right), \\ \bar{P}_{13} &= -\bar{D}\left(\frac{\partial^2}{\partial y^2} + \nu\frac{\partial^2}{\partial x^2}\right), \\ \bar{P}_{14} &= -\bar{D}(1-\nu)\frac{\partial^2}{\partial x \partial y}, \\ \bar{P}_{22} &= \bar{P}_{33} = -\bar{D}, \\ \bar{P}_{23} &= \bar{P}_{32} = -\nu\bar{D}, \\ \bar{P}_{44} &= -\frac{1}{2}\bar{D}(1-\nu), \\ \bar{u}_2 &= \frac{\bar{M}_x - \nu\bar{M}_y}{\bar{D}(1-\nu^2)}, \end{aligned} \tag{A.2}$$

$$\bar{u}_3 = \frac{\bar{M}_y - \nu \bar{M}_x}{\bar{D}(1-\nu^2)},$$

$$\bar{u}_4 = \frac{2\bar{M}_{xy}}{\bar{D}(1-\nu)}.$$

The Gateaux derivative of the operator is the following vector:

$$d\,\bar{\boldsymbol{Q}}\left(\bar{\boldsymbol{u}}, \bar{\boldsymbol{u}}^*\right) = \begin{bmatrix} -\frac{\partial^2 \bar{M}_x^*}{\partial x^2} - \frac{\partial^2 \bar{M}_y^*}{\partial y^2} - 2\frac{\partial^2 \bar{M}_{xy}^*}{\partial x \partial y} \\ -\bar{M}_x^* - \bar{D}\left(\frac{\partial^2 \bar{w}^*}{\partial x^2} + \nu \frac{\partial^2 \bar{w}^*}{\partial y^2}\right) \\ -\bar{M}_y^* - \bar{D}\left(\frac{\partial^2 \bar{w}^*}{\partial y^2} + \nu \frac{\partial^2 \bar{w}^*}{\partial x^2}\right) \\ -\bar{M}_{xy}^* - (1-\nu)\bar{D}\frac{\partial^2 \bar{w}^*}{\partial x \partial y} \\ \bar{T}^* \\ -\bar{M}^* \\ \bar{w}^{*\prime} \\ -\bar{w}^* \end{bmatrix}. \tag{A.3}$$

References

Aköz, A.Y., Kadıoğlu, F.: The mixed finite element method for the quasi-static and dynamic analysis of viscoelastic Timoshenko beams. Int. J. Numer. Methods Eng. **44**, 1909–1932 (1999)

Aköz, A.Y., Özçelikörs, Y.: A new functional for plates and a new finite element formulation. In: Proc. on the 9th National Applied Mechanics Meeting, Turkish, Bayramoğlu-Kocaeli, pp. 113–123 (1985)

Aköz, A.Y., Özütok, A.: A functional for shells of arbitrary geometry and a mixed finite element method for parabolic and circular cylindrical shells. Int. J. Numer. Methods Eng. **47**, 1933–1981 (2000)

Aral, M.M., Gülçat, Ü.: A finite element Laplace transform solution technique for wave equation. Int. J. Numer. Methods Eng. **11**, 1719–1732 (1977)

Bathe, K.J.: Finite Element Procedures in Engineering Analysis. Prentice-Hall, Englewood Cliffs (1982)

Chen, T.: The hybrid Laplace transform/finite element method applied to the quasi-static and dynamic analysis of viscoelastic Timoshenko beams. Int. J. Numer. Methods Eng. **38**, 509–522 (1995)

Christensen, R.M.: Theory of Viscoelasticity, 2nd edn. Academic Press, New York (1982)

Craig, R.R. Jr, Kurdila, A.J.: Fundamentals of Structural Dynamics, 2nd edn. Wiley, New York (2006)

Dubner, H., Abate, J.: Numerical inversion of Laplace transforms by relating them to the finite Fourier cosine transform. J. ACM **15**, 115–123 (1968)

Durbin, F.: Numerical inversion of Laplace transforms: an efficient improvement to Dubner and Abate's method. Comput. J. **17**, 371–376 (1974)

Dym, C.L., Shames, I.H.: Solid Mechanics: A Variational Approach. McGraw-Hill, New York (1973)

Flügge, W.: Viscoelasticity, 2nd edn. Springer, Berlin (1975)

Huebner, K.H.: The Finite Element Method for Engineers. Wiley, New York (1975)

Ilioushin, A.A., Pobedria, B.E.: Fundamentals of the Mathematical Theory of Thermoviscoelasticity. Nauka, Moscow (1970)

Ilyasov, M.H., Aköz, A.Y.: The vibration and dynamic stability of viscoelastic plates. Int. J. Eng. Sci. **38**, 695–714 (2000)

Kadıoğlu, F., Aköz, A.Y.: The mixed finite element method for the dynamic analysis of visco-elastic circular beams. In: Proc. of the 4th International Conference on Vibration Problems, Jadavpur University (1999)

Kadıoğlu, F., Aköz, A.Y.: The quasi-static and dynamic responses of viscoelastic parabolic beams. In: Proc. on the 11th National Applied Mechanics Meeting, Turkish, Bolu-Turkey (2000)

Kadıoğlu, F., Aköz, A.Y.: The mixed finite element for the quasi-static and dynamic analysis of viscoelastic circular beams. Int. J. Struct. Eng. Mech. **15**, 735–752 (2003)

Krylov, V.I., Skoblya, N.S.: Handbook of numerical inversion of Laplace transforms. Translated from Russian, Israel Program for Scientific Translations, Jerusalem (1969)

Leissa, A.W.: Vibration of Plates. NASA SP-160. US Government Printing Office, Washington, DC (1969)

Lovadina, C.: A new class of mixed finite element methods for Reissner–Mindlin plates. SIAM J. Numer. Anal. **33**, 2457–2467 (1996)
Narayanan, G.V., Beskos, D.E.: Numerical operational methods for time-dependent linear problems. Int. J. Numer. Methods Eng. **18**, 1829–1854 (1982)
Oden, J.T., Reddy, J.N.: Variational Methods in Theoretical Mechanics. Springer, Berlin (1976)
Reddy, J.N.: An Introduction to the Finite Element Method, 2nd edn. McGraw-Hill, New York (1993)
Sorvari, J., Hämäläinen, J.: Time integration in linear viscoelasticity—a comparative study. Mech. Time-Depend. Mater. **14**, 307–328 (2010)
Temel, B., Şahan, M.F.: An alternative solution method for the damped response of laminated Mindlin plates. Composites, Part B, Eng. **47**, 107–117 (2013)
Timoshenko, S.P., Woinowsky-Krieger, S.: Theory of Plates and Shells. McGraw-Hill, New York (1959)
Wang, J., Birgisson, B.: A time domain boundary element method for modeling the quasi-static viscoelastic behavior of asphalt pavements. Eng. Anal. Bound. Elem. **31**, 226–240 (2007)
Wang, Y.Z., Tsai, T.J.: Static and dynamic analysis of a viscoelastic plate by the finite element method. Appl. Acoust. **25**, 77–94 (1988)
White, J.L.: Finite elements in linear viscoelastic analysis. In: Proc. of the 2nd Conference on Matrix Method in Structural Mechanics. AFFDL-TR-68-150, pp. 489–516 (1986)
Xu, Q., Rahman, M.S., Tayebali, A.A.: A finite element analysis of layered viscoelastic system under vertical circular loading. Numer. Methods Geomech. **9**, 479–486 (2004)
Yi, S., Hilton, H.H.: Dynamic finite element analysis of viscoelastic composite plates. Int. J. Numer. Methods Eng. **37**, 4081–4096 (1994)